

Article

# The Overmaraat-Gol Alkaline Pluton in Northern Mongolia: U–Pb Age and Preliminary Implications for Magma Sources and Tectonic Setting

Vassily V. Vrublevskii <sup>1,\*</sup>, Igor F. Gertner <sup>1</sup>, Richard E. Ernst <sup>1,2</sup>, Andrey E. Izokh <sup>1,3,4</sup>  
and Andrey V. Vishnevskii <sup>1,3,4</sup>

<sup>1</sup> Department of Geology and Geography, Tomsk State University, Tomsk 634050, Russia; labspm@ggf.tsu.ru (I.F.G.); richard.ernst@ernstgeosciences.com (R.E.E.); izokh@igm.nsc.ru (A.E.I.); vishnevsky@igm.nsc.ru (A.V.V.)

<sup>2</sup> Department of Earth Sciences, Carleton University, Ottawa, ON K1S 5B6, Canada

<sup>3</sup> Institute of Geology and Mineralogy, Siberian Branch of the Russian Academy of Sciences, Novosibirsk 630090, Russia

<sup>4</sup> Department of Geology and Geophysics, Novosibirsk State University, Novosibirsk 630090, Russia

\* Correspondence: vasvr@yandex.ru; Tel.: +7-3822-529-749

Received: 11 January 2019; Accepted: 6 March 2019; Published: 10 March 2019



**Abstract:** A new Wenlockian zircon U–Pb age (~426 Ma) of the Overmaraat-Gol nepheline syenite (foyaite, juvite) pluton in the SW Lake Hovsgol area (Northern Mongolia) prompts a long history of alkaline magmatism in the western Central Asian Orogenic Belt, exceeding the duration of the Devonian and Permian–Triassic events. The LILE and HFSE patterns of pluton samples analyzed by X-ray fluorescence (XRF) and inductively coupled plasma (ICP-MS) methods indicate intrusion in a complex tectonic setting during interaction of a mantle plume with accretionary-collisional complexes that previously formed on the active continental margin. As a result, the parent magma had a heterogeneous source with mixed mantle (PREMA and EM) and crustal components. This source composition is consistent with Nd–Sr isotope ratios of the Overmaraat-Gol alkaline rocks, from  $-0.1$  to  $-1.2 \epsilon_{\text{Nd}}(t)$  and from  $\sim 0.706$  to  $0.707$   $^{87}\text{Sr}/^{86}\text{Sr}(t)$ .

**Keywords:** alkaline magmatism; geochemistry; U–Pb isotope geochronology; plume–lithosphere interaction; Northern Mongolia; Central Asian Orogenic Belt

## 1. Introduction

Main events of continental and marine alkaline magmatism are often coeval with the activity pulses of mantle plumes [1,2]. This synchronicity is evident in within-plate settings, but is often obscured in orogenic belts where supracrustal contamination masks the true magma sources [3–11]. The plume–lithosphere interaction can produce hybrid magmas with high  $\text{Al}_2\text{O}_3$  contents and induce the formation of nepheline-enriched plutonic rocks. Constraints on ages and trace-element compositions of alkaline intrusions in fold belts have important implications for their origin.

Feldspathoid-rich (foiolites, nepheline syenites) igneous rocks in the western Central Asian Orogenic Belt (CAOB) are mostly from the Paleozoic ages. Such magmatism culminated at 520–470 Ma, 405–385 Ma, and 310–260 Ma in the northeastern Kuznetsk Alatau, western Baikal, western Transbaikalia, southeastern Tuva, and southeastern Russian Altai regions [5,7,12–16] (Figure 1a). Judging by their petrography, the rocks mostly belong to a differentiated magma series of subalkaline gabbro and theralite–foiolite–nepheline and alkaline syenite. In Northwestern Mongolia, igneous rocks of this composition form several plutons in the southwestern Hovsgol area [17]. The largest plutons (Overmaraat-Gol, Beltesin-Gol, Duchin-Gol, and Serheul intrusions) are controlled by a

regional fault (Figure 1b). Previous time constraints were limited to poorly reliable 396–400 Ma (Devonian) K–Ar ages obtained for nepheline and mica [13]. The available U–Pb ages for the Overmaraat-Gol pluton indicate that the magma intruded during the Early Silurian. Unlike the widespread Devonian and Permian–Triassic alkaline magmatism, the earlier intrusion may have been the final phase (“last echo”) of the Early Paleozoic North-Asian mantle plume [18]. The trace-element chemistry and isotope systematics of the Overmaraat-Gol igneous rocks indicate a mixed mantle-crust source of the parent alkaline-mafic magma, which possibly generated and intruded during the interaction of a mantle plume with older, active continental margin accretionary–collisional complexes.

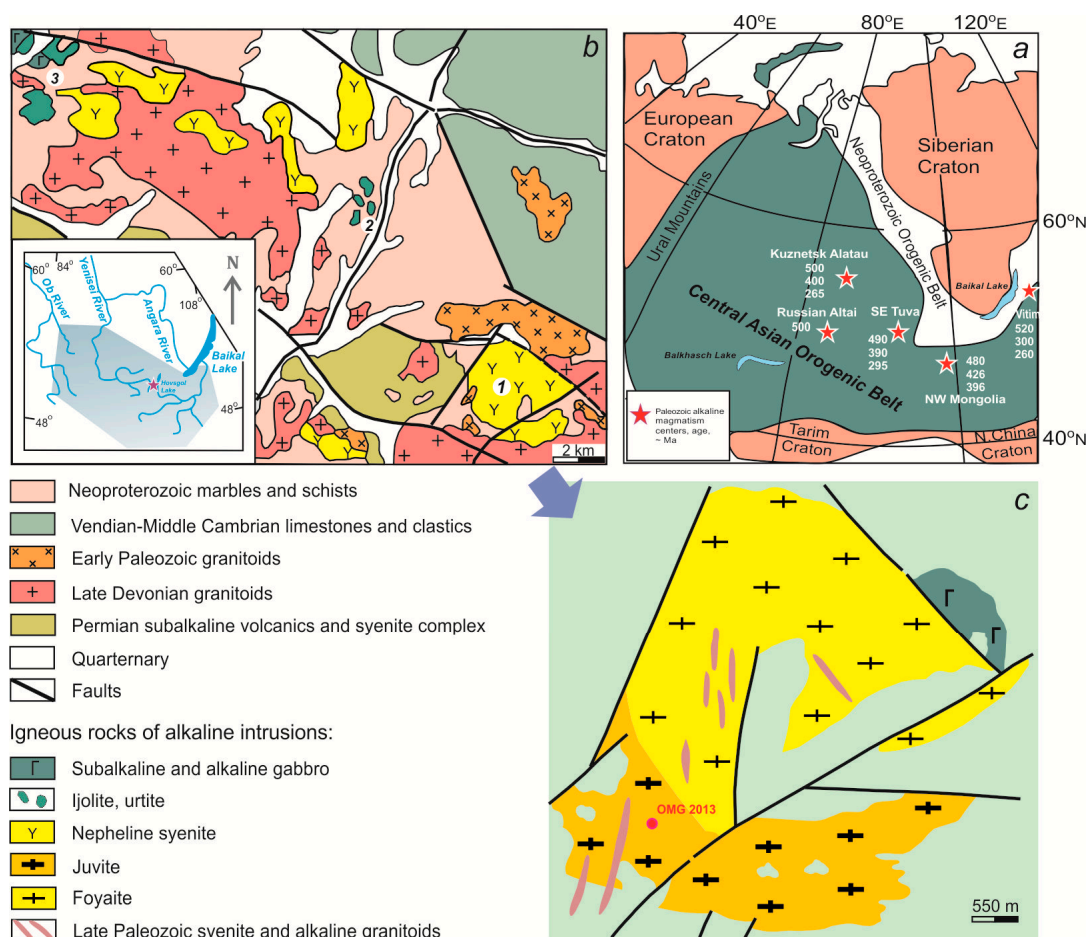


**Figure 1.** (a) Location map of Paleozoic carbonatite–alkaline intrusive complexes in the western Central Asian Orogenic Belt, simplified after [19,20]; (b) tectonic framework of alkaline intrusions in the SW Hovsgol area of Northern Mongolia: Overmaraat-Gol ((1) dark pink star in the inset); Duchin-Gol (2); Beltesin-Gol (3), after [13,21]. Grey area in the inset shows the Early Paleozoic large igneous province [7]; (c) simplified geology of the Overmaraat-Gol pluton, after [13]. OMG 2013 was the sample for U–Pb dating.

## 2. Geology and Petrography of the Overmaraat-Gol Intrusion

The studied intrusions are located in the SW Hovsgol area, within a fault-bounded block of the Precambrian Tuva-Mongolia terrane in the middle of the Central Asian Orogenic Belt [22]. The terrane has a Neoproterozoic basement of marbles and schists derived from Vendian–Cambrian continental-margin metacarbonate and clastic sediments. The Overmaraat-Gol pluton and related alkaline plutons in the Beltesin-Gol–Udgigin-Gol interfluvium follow an N–S backbone fault [13,21]. The intrusions crosscut basement marbles and Early Paleozoic gabbro-diorites and granitoids (Figure 1b).

The Overmaraat-Gol pluton, exposed over 30 km<sup>2</sup> on the erosion surface, has an isometric shape in the map view and consists of several blocks (Figure 1c). The rocks comprise main petrographic varieties of coarse-grained K–Na nepheline syenite (foyaite and juvite for brevity), transient from one to another, with variable amounts of nepheline, feldspars (microcline and albite), and femic minerals (aegirine-salite-hedenbergite, aegirine-augite, sodic and sodic-calcic amphiboles—arfvedsonite and katophorite-hastingsite) [13]. Older subalkaline gabbro and theralites are preserved only as small xenolith-like bodies. Secondary alteration of igneous rocks has produced lepidomelane, muscovite, and cancrinite. Juvites and foyaite are crosscut by Devonian syenite and leucogranite dikes [21], which does not contradict the obtained U–Pb age of alkaline intrusions.

### 3. Analytical Methods

Major elements in rocks were analyzed by X-ray fluorescence (XRF) on a Thermo Scientific ARL 9900XP spectrometer at the V.S. Sobolev Institute of Geology and Mineralogy (Novosibirsk). Trace-element and REE abundances were measured by mass spectrometry with inductively coupled plasma (ICP-MS) on an Agilent 7500cx spectrometer under standard operation conditions, at the Analytical Center of Geochemistry of Natural Systems at the Tomsk National Research State University (Tomsk, Russia).

Zircon U–Pb ages were determined on a SHRIMP-II ion microprobe at the Center of Isotope Studies of the A.P. Karpinsky Russian Geological Research Institute (St. Petersburg, Russia), following the standard procedure [23]. Cathodoluminescence (CL) images were obtained on an ABT55 scanning electron microscope in the conventional operation mode. Data were processed using SQUID software (Version 1.00) [24]. U/Pb ratios were normalized to those in the TEMORA standard zircon [25]. The errors were within  $\pm 1\sigma$  in measured isotope ratios and ages, but  $\pm 2\sigma$  in calculated concordant ages and intersections with concordia. Concordia diagrams were plotted in ISOPLOT/Ex (Version 2.10) [26].

Sm–Nd and Rb–Sr isotope analyses were carried out by the standard technique [27] on the Finnigan MAT-262 and MI 1201-T mass spectrometers at the Geological Institute of the Kola Science Center (Apatity, Russia). The  $\epsilon_{Nd}$  and  $\epsilon_{Sr}$  values, and primary Nd and Sr isotope ratios were used for reference in calculations of U–Pb zircon ages (see text), assuming modern CHUR  $^{143}Nd/^{144}Nd = 0.512638$ ,  $^{147}Sm/^{144}Nd = 0.1967$ ; UR  $^{87}Sr/^{86}Sr = 0.7045$ ,  $^{87}Rb/^{86}Sr = 0.0827$  [28]. The contents of the elements were determined by isotope dilution to an accuracy of 0.5 rel. % for Sm and Nd, and 1 rel. % for Rb and Sr. Measurements for the La Jolla standard sample yielded the average ratio,  $^{143}Nd/^{144}Nd = 0.511851$  (N = 20).  $^{87}Sr/^{86}Sr$  ratios were normalized to the value of 0.710235 of NBS SRM-987.

### 4. Results

#### 4.1. Major- and Trace-Element Compositions of Alkaline Rocks

The analyzed predominant feldspathoid-bearing rocks typically had variable silica contents (48–57 wt % SiO<sub>2</sub>) and high contents of alkalis (up to 12–16.5 wt % Na<sub>2</sub>O + K<sub>2</sub>O; Na<sub>2</sub>O/K<sub>2</sub>O  $\approx$  1.2–2.8) and alumina (20–31 wt % Al<sub>2</sub>O<sub>3</sub>), which are common to products of K–Na mafic alkaline magmatism. Rocks with higher feldspar percentages had nepheline-bearing alkaline syenite-pulaskite compositions with up to 63 wt % SiO<sub>2</sub> (Table 1; Figure 2a,b). As silica increased, the changes in the other major oxides remained moderate—from 0.7 wt % to 2 wt % CaO, 0.1 wt % to 0.7 wt % MgO, 1.3 wt % to 5 wt % Fe<sub>2</sub>O<sub>3</sub> and 0.1 wt % to 0.4 wt % TiO<sub>2</sub>. The respective ranges of compatible elements were 6–10 ppm Cr, 5–18 ppm Ni, 0.9 to 5–18 ppm Co, 0.8 to 6.5 ppm V, and 0.4–1 ppm Sc.

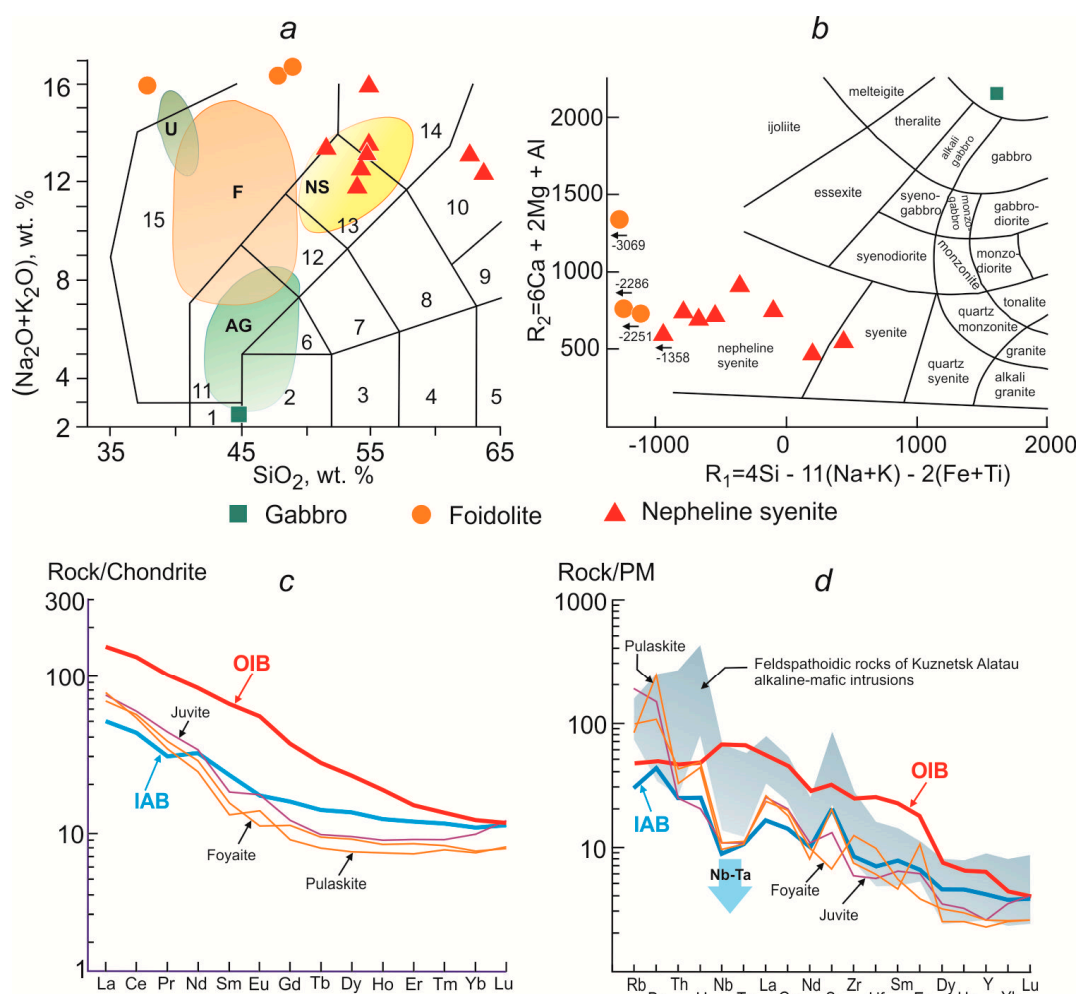


**Figure 2.** Classification and composition of the Overmaraat-Gol alkaline rocks: (a) Total alkalis vs. silica (TAS) diagram [29]. 1 = peridotite gabbro, 2 = subalkaline gabbro, 3 = gabbro-diorite, 4 = diorite, 5 = granodiorite, 6 = monzogabbro, 7 = monzodiorite, 8 = monzonite, 9 = quartz-monzonite, 10 = syenite, 11 = nepheline gabbro, 12 = nepheline monzodiorite, 13 = nepheline monzosyenite, 14 = nepheline syenite, 15 = foidolite; (b)  $R_1$ – $R_2$  diagram [30]. Diagrams in panels (a,b) include new representative analyses (Table 1) and published data from [13,21]. Fields of different colors mark predominant compositions of Paleozoic sudalkaline and alkaline gabbro (AG), foidolites (F), urtites (U), and nepheline syenites (NS) in the northern Kuznetsk Alatau province; (c,d) chondrite-normalized [31] REE patterns (c) and PM-normalized [31] multi-element diagram (d). Average ocean island basalt (OIB) and island-arc basalt (IAB) compositions are after Sun and McDonough (1989) [31] and Kelemen et al. (2003) [32], respectively.

Only Rb (53–115 ppm) and Ba (756–1692 ppm) contents reached (or exceeded) the average level for ocean island basalt (OIB), while Th (2–3.6 ppm) and U (0.4–1 ppm) approached this level more or less closely. HFSE patterns with 7–8 ppm Nb, 0.4–0.5 ppm Ta, 66–146 ppm Zr, 1.7–3 ppm Hf, 75–85 ppm REE, and 139–416 ppm Sr were similar to those in island-arc basalt (IAB), and bore evidence of magma evolution in an active continental margin setting (Table 1, Figure 2c,d). Nb–Ta showed a prominent minimum as a record of a subduction component [32].

Table 1. Representative analyses of Overmaraat-Gol alkaline rocks.

Rock Type	Juvite			Pulaskite			Rock Type	Juvite			Pulaskite				
Sample	1–10	5–9	2–12	Sample	1–10	5–9	2–12	Sample	1–10	5–9	2–12	Sample	1–10	5–9	2–12
SiO <sub>2</sub> , wt %	51.54	62.97	63.33	Sr	279	139	416	Sr	279	139	416	Sr	279	139	416
TiO <sub>2</sub>	0.29	0.11	0.18	Nb	7.5	8	6.8	Nb	7.5	8	6.8	Nb	7.5	8	6.8
Al <sub>2</sub> O <sub>3</sub>	26.38	20.67	19.64	Ta	0.46	0.5	0.44	Ta	0.46	0.5	0.44	Ta	0.46	0.5	0.44
Fe <sub>2</sub> O <sub>3</sub>	4.57	1.34	2.63	Zr	66	146	83	Zr	66	146	83	Zr	66	146	83
MnO	0.09	0.02	0.05	Hf	1.7	3	1.9	Hf	1.7	3	1.9	Hf	1.7	3	1.9
MgO	0.35	0.07	0.13	Y	12	12	10	Y	12	12	10	Y	12	12	10
CaO	1.96	0.69	1.47	Th	2	3.6	2.6	Th	2	3.6	2.6	Th	2	3.6	2.6
Na <sub>2</sub> O	8.45	7.47	6.73	U	0.42	1	0.9	U	0.42	1	0.9	U	0.42	1	0.9
K <sub>2</sub> O	4.85	5.57	5.56	La	17	16	18	La	17	16	18	La	17	16	18
P <sub>2</sub> O <sub>5</sub>	0.11	0.08	0.05	Ce	36	35	31	Ce	36	35	31	Ce	36	35	31
LOI	1.09	0.47	0.05	Pr	4	3.5	3	Pr	4	3.5	3	Pr	4	3.5	3
Total	99.68	99.46	99.82	Nd	15	13	11	Nd	15	13	11	Nd	15	13	11
Na <sub>2</sub> O + K <sub>2</sub> O	13.30	13.04	12.29	Sm	2.8	2.4	2	Sm	2.8	2.4	2	Sm	2.8	2.4	2
Na <sub>2</sub> O/K <sub>2</sub> O	1.74	1.34	1.21	Eu	1	0.64	0.8	Eu	1	0.64	0.8	Eu	1	0.64	0.8
Cr, ppm	9	10	6	Gd	2.5	2.2	1.9	Gd	2.5	2.2	1.9	Gd	2.5	2.2	1.9
Ni	2.7	3	5	Tb	0.39	0.37	0.31	Tb	0.39	0.37	0.31	Tb	0.39	0.37	0.31
V	1.2	0.8	2.5	Dy	2.4	2.3	1.9	Dy	2.4	2.3	1.9	Dy	2.4	2.3	1.9
Co	3	0.9	2	Ho	0.51	0.48	0.42	Ho	0.51	0.48	0.42	Ho	0.51	0.48	0.42
Sc	0.4	0.4	1	Er	1.5	1.4	1.2	Er	1.5	1.4	1.2	Er	1.5	1.4	1.2
Cs	6.4	0.61	0.35	Tm	0.23	0.21	0.2	Tm	0.23	0.21	0.2	Tm	0.23	0.21	0.2
Rb	115	63	53	Yb	1.7	1.3	1.3	Yb	1.7	1.3	1.3	Yb	1.7	1.3	1.3
Ba	1086	756	1692	Lu	0.3	0.2	0.2	Lu	0.3	0.2	0.2	Lu	0.3	0.2	0.2

The behavior of REE (Figure 2c) likewise indicates an IAB contribution. The LREE/HREE ratios are moderate ( $\approx 7.2$ – $8.3$ ); the  $\text{Eu}/\text{Eu}^* \approx 0.8$ – $1.3$  and  $(\text{La}/\text{Yb})_N \approx 7.2$ – $10$  ratios are similar to those in average OIB (1.05 and 12.3, respectively).

#### 4.2. Nd–Sr Isotope Systematics

Juvite and pulaskite in the area shared similarities in primary Nd isotope ratios of  $^{143}\text{Nd}/^{144}\text{Nd}(t) = 0.512028$ – $0.512085$  and  $\epsilon_{\text{Nd}}(t)$  from  $-1.2$  to  $-0.1$  (Table 2), and thus may have originated from the same magma source, where moderately depleted (PREMA-type) mantle was mixed with an enriched (EM-type) component. On the other hand, inputs of crustal material were recorded in Sr isotope ratios of  $^{87}\text{Sr}/^{86}\text{Sr}(t) = 0.70597$ – $0.70706$  and  $\epsilon_{\text{Sr}}(t) = 28$ – $43$  (Table 2; Figure 3), as well as in the oxygen isotope composition of  $7.9$ – $10.6\text{‰}$   $\delta^{18}\text{O}_{\text{SMOW}}$  which was higher than in the mantle [3]. Enrichment in supracrustal  $^{87}\text{Sr}$  was reported for many Paleozoic–Mesozoic alkaline and carbonatite complexes in the western CAOB [3–9,11,12,33], where lithospheric substrate could interact with EM material.

Table 2. Nd–Sr isotope compositions of alkaline rocks, Overmaraat-Gol pluton.

Sample, Rock	Sm, ppm	Nd, ppm	$^{147}\text{Sm}/^{144}\text{Nd}$	$^{143}\text{Nd}/^{144}\text{Nd}$	$\pm 2\sigma$	$^{143}\text{Nd}/^{144}\text{Nd}(t)$	$\epsilon_{\text{Nd}}(t)$
1–10, juvite	2.78	15.3	0.10991	0.512391	7	0.512085	−0.1
5–9, pulaskite	2.61	14.1	0.11199	0.512340	5	0.512028	−1.2
Sample, Rock	Rb, ppm	Sr, ppm	$^{87}\text{Rb}/^{86}\text{Sr}$	$^{87}\text{Sr}/^{86}\text{Sr}$	$\pm 2\sigma$	$^{87}\text{Sr}/^{86}\text{Sr}(t)$	$\epsilon_{\text{Sr}}(t)$
1–10, juvite	121.2	315.9	1.082474	0.71362	18	0.70706	+43.4
5–9, pulaskite	66.15	143.2	1.283619	0.71375	14	0.70597	+28.0

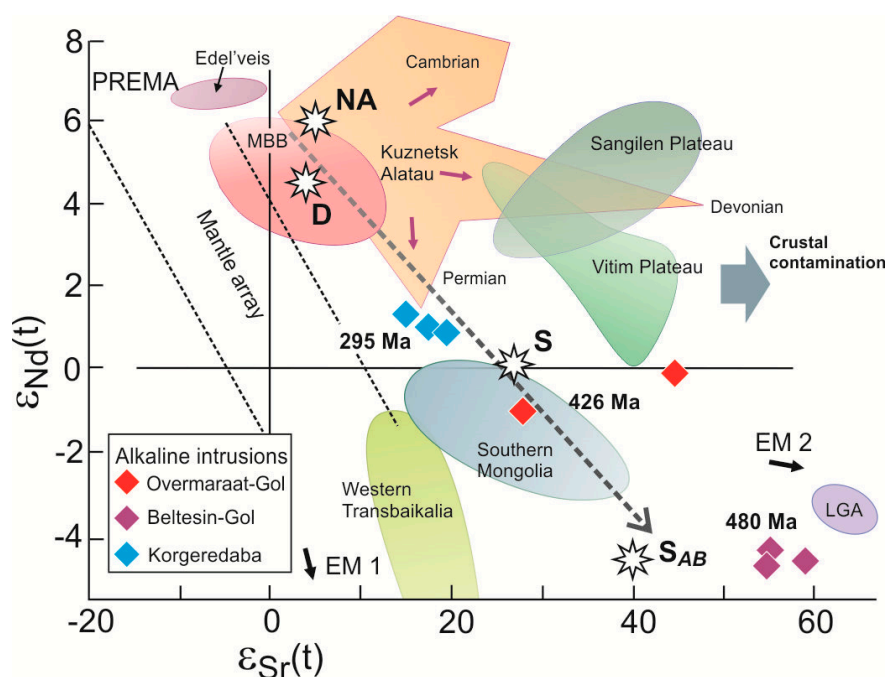


**Figure 3.**  $\epsilon_{Nd}(t)$  vs.  $\epsilon_{Sr}(t)$  plot for the Overmaraat-Gol pluton and some other alkaline complexes from the western Central Asian Orogenic Belt: Paleozoic intrusions of the Sangilen Plateau, Vitim Plateau, Russian Altai (complex Edelveis), Kuznetsk Alatau, and basalts of the Minusa Basin (MBB), after [5–9,11,33,34]. Korgeredaba nepheline syenites (~295 Ma, SE Tuva), after [35,36] and Beltesin-Gol carbonatites (~480 Ma, Northern Mongolia), after [37,38]; Mesozoic intrusions of Southern Mongolia (Mushgai Khudag, Bayan Khoshuu), Western Transbaikalia (Oshurkovo, Arshan, Khaluta) and lamproites of the Russian Altai, after [37,39–41]. White stars are average compositions of the North Asian (NA), Devonian (D), and Siberian (S, AB = alkali basalts) mantle plumes, after [18,34,42]. Dash line shows composition trend of the plume component. “Mantle array” domain and PREMA, EM 1, and EM 2 modern mantle reservoirs are according to [43,44].

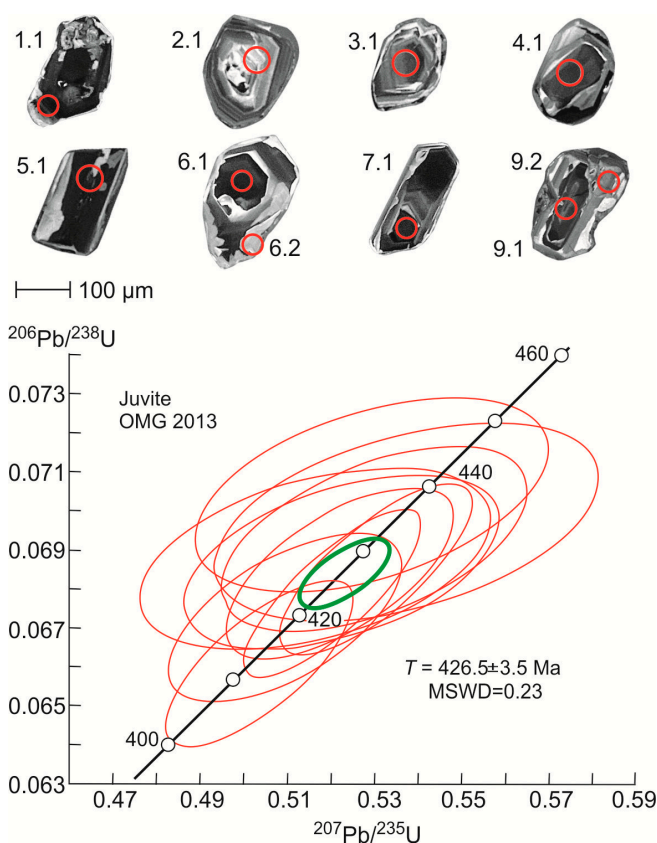
#### 4.3. U–Pb Zircon Dating

The age of the Overmaraat-Gol pluton was determined by U–Pb dating of eight accessory zircons from a juvite sample (OMG 2013, Table 3). They were dipyrmid-prismatic crystals with oscillatory zoning, or crystal chips with Th and U contents, which varied notably even within single grains and Th/U ratios from 0.1 to 1.1. The whole zircon population showed a concordant age of  $426.5 \pm 3.5$  Ma (Figure 4), which may correspond to the time of magma emplacement. Some grains had reverse zonation with a  $\approx 5$ –15 Ma difference between core and rim (points 6.1, 6.2, 9.1, and 9.2 in Figure 4), possibly, as a result of lead loss upon hydrothermal leaching of alkaline igneous rocks [45]. The contents of U, Th, and radiogenic  $^{206}\text{Pb}$  in the zoned grains decreased markedly from core to rim. Reverse zonation was also reported for zircons in juvite from the Kurgusul pluton in the Kuznetsk Alatau [12]. A close age of  $\sim 425$ – $435$  Ma was inferred for some granitoids in the Kuznetsk Alatau and Sayan areas [46,47]. Similar Paleozoic alkaline-mafic intrusions in the western CAOBE emplaced in discrete events at  $\sim 500$ ,  $\sim 400$ , and  $\sim 300$  Ma, which did not overlap with the U–Pb age of this study [6–8,12,14,15].

**Table 3.** Results of SHRIMP-II U–Pb zircon dating of juvite (sample OMG 2013) from the Overmaraat-Gol pluton.

Points	$^{206}\text{Pb}_c$ , %	U, ppm	Th, ppm	$^{232}\text{Th}/^{238}\text{U}$	$^{206}\text{Pb}^*$ , ppm	$^{206}\text{Pb}/^{238}\text{U}$ Age, Ma	$^{207}\text{Pb}^*/^{235}\text{U}$ $\pm\%$	$^{206}\text{Pb}^*/^{238}\text{U}$ $\pm\%$	Rho
1.1	0.13	1478	1654	1.16	87.1	$427.2 \pm 7.7$	$0.5304 \pm 1.7$	$0.0685 \pm 1.3$	0.768
2.1	0.30	241	87	0.37	14.5	$434.5 \pm 6.3$	$0.537 \pm 3.3$	$0.0697 \pm 1.5$	0.446
3.1	0.49	526	254	0.50	31.2	$428.7 \pm 5.7$	$0.516 \pm 3.2$	$0.0688 \pm 1.4$	0.432
4.1	0.28	982	139	0.15	58.1	$428.2 \pm 5.5$	$0.522 \pm 2.8$	$0.0687 \pm 1.3$	0.469
5.1	0.09	1141	492	0.45	64.8	$412.5 \pm 5.3$	$0.5037 \pm 1.7$	$0.0661 \pm 1.3$	0.753
6.1 core	0.07	1726	1190	0.71	101	$423.3 \pm 5.3$	$0.5204 \pm 1.6$	$0.0679 \pm 1.3$	0.811
6.2 rim	0.28	308	29	0.10	18.7	$438.7 \pm 6.1$	$0.529 \pm 3.1$	$0.0704 \pm 1.4$	0.461
7.1	0.61	1382	1157	0.86	80.4	$419.6 \pm 5.3$	$0.51 \pm 2.1$	$0.0673 \pm 1.3$	0.614
9.1 core	0.19	587	289	0.51	34.5	$426.6 \pm 5.4$	$0.522 \pm 2$	$0.0684 \pm 1.3$	0.643
9.2 rim	0.23	314	114	0.37	18.7	$431.8 \pm 5.8$	$0.53 \pm 2.7$	$0.0693 \pm 1.4$	0.519

Note:  $\text{Pb}_c$  and  $\text{Pb}^*$  are common and radiogenic lead, respectively. Correction for common lead was made using measured  $^{204}\text{Pb}$ . Rho is the coefficient of correlation between the errors of measurement of  $^{235}\text{U}/^{207}\text{Pb}$  and  $^{238}\text{U}/^{206}\text{Pb}$ .

**Figure 4.** U–Pb concordia diagram for zircons from the Overmaraat-Gol juvite (sample OMG 2013): Morphology and structure of zircon crystals according to cathodoluminescence data. Circles are sites of isotope analysis, with number of analyzed grains (Table 3).

## 5. Discussion

### 5.1. Magma and Rock Sources

The evolution of alkaline and carbonatite magmatism is often attributed to the activity of mantle plumes which drain HIMU/FOZO [44] reservoirs and interact with EM 1 material [48]. Products of nephelinite volcanism may differ in Nd and Sr systematics even in coeval and spatially proximal volcanic centers, as it was shown for the East African rift [48]. The Nd isotope composition, with  $-1.2$  to  $-0.1$   $\epsilon_{\text{Nd}}(t)$ , indicated that the parent melts of the Overmaraat-Gol rocks originated at mantle depths

and contained a PREMA plume component and a major contribution of EM-type enriched lithospheric mantle material (Figure 3). Isotope heterogeneity results from differences in the relative percentages of material from different reservoirs more or less strongly mixed in the magma source. Like the case of volcanic rocks from Italy [49], the isotope geochemistry of the Overmaraat-Gol igneous rocks may correlate with melt fraction in moderately depleted mantle mixed with the material of an ITEM-like mantle source containing  $^{87}\text{Sr}$  markedly above the OIB level. On the other hand, continental crust inputs to the sublithospheric upper mantle may have contributed to the origin of such a mantle domain.

Although bearing signatures of mantle origin, the rocks had quite high ratios of  $^{87}\text{Sr}/^{86}\text{Sr}$  ( $\approx 0.706\text{--}0.707$ ) and  $\delta^{18}\text{O}$  ( $\approx 8\text{--}11\%$ ) [3], corresponding to supracrustal material.  $^{87}\text{Sr}$  may come from brines that were preserved in sediments and mobilized by the hot intrusions [3,6]. Crustal contamination may account for the lack of correlation between the Nd and Sr isotope compositions and for the magma evolution within the mantle array (Figure 3). Similar signatures of interaction were reported for many alkaline and carbonatite plutonic complexes of different ages in the western CAO (Figure 3). Simultaneous involvement of EM-type and mature continental crust material was inferred for Mesozoic intrusions in areas of thick lithosphere, such as Western Transbaikalia, Southern Mongolia, and Russian Altai [4,40,41], but not in the southwestern Hovsgol area and the Sangilen Plateau in southeastern Tuva (Korgeredaba pluton). Therefore, magma sources may differ even in adjacent areas.

General similarity in the isotope evolution of alkaline magmatism in the western CAO suggests a genetic relationship of magma sources and plume–lithosphere interaction in the same tectonic setting. Given that the history of magmatism comprised several events of different ages, it is reasonable to hypothesize that the igneous rocks inherited isotope signatures from remolten lower lithosphere material metasomatized by the initial plume [12]. The predominant PREMA component in mafic magmas was noted previously in the context of the Paleozoic history of the North-Asian superplume [18].

### *5.2. Tectonic Setting of the Overmaraat-Gol Intrusion and Its Place in the History of Alkaline Magmatism in the Western CAO*

The patterns of trace elements from the Overmaraat-Gol pluton record heterogeneous sources and a complex tectonic setting of alkaline magmatism. Although REE in the igneous rocks show similar fractionation degrees ( $\text{La}/\text{Yb}_N \sim 7\text{--}10$ ), most HFSE have contents commensurate with the average values for IAB, which are consistent with higher element concentrations in the Middle Cambrian–Devonian fooidic intrusions from the Kuznetsk Alatau (Figure 2c,d). Relatively high contents of Rb and Ba, as well as Th and U, may record an OIB contribution associated with a mantle plume. The positive Eu-anomaly ( $\text{Eu}/\text{Eu}^* = 1.2\text{--}1.3$ ) provides implicit evidence for an originally large depth of magma generation. The behavior of HFSE corresponds to magma evolution in an active continental margin setting. The inheritance of geochemical signatures from earlier subduction magmatism was discussed previously for alkaline rocks, as well as for Early Paleozoic granitic and gabbro-monzonitic rocks intruding the accretionary-collisional complexes of the Cambrian Kuznetsk–Altai island arc in the western CAO [6,7,46,50]. Likewise, the alkaline intrusions of Northern Mongolia may have formed during migration of a mantle plume in the ocean-to-continent transition zone.

The heterogeneity of material was further confirmed by variations in the  $\text{Th}/\text{Yb}\text{--}\text{Ta}/\text{Yb}$ ,  $\text{Th}_N\text{--}\text{Nb}_N$ , and  $\text{Nb}/\text{Y}\text{--}\text{Zr}/\text{Y}$  ratios, which either corresponded to the plume/non-plume discrimination line for magma sources (Figure 5c), or converged with the fields of within-plate and continental-margin basaltic rocks (Figure 5a,b,d). This similarity was not fortuitous and may have resulted from the interaction of plume material with older accretionary-collisional complexes on the active margin of the Paleasian ocean. The contribution of mature continental crust to the magma sources was consistent with the probable age, geochemistry, and isotope systematics of the Overmaraat-Gol rocks.

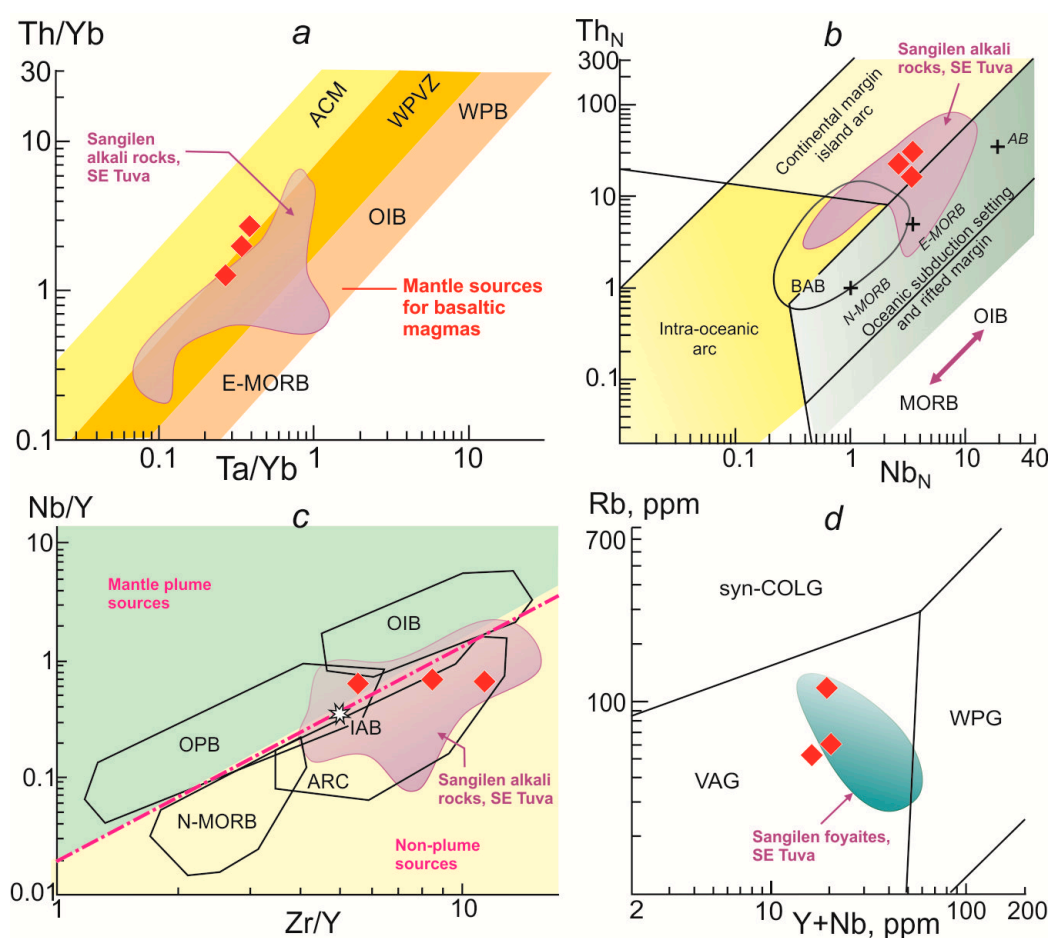


**Figure 5.** HFSE in the Overmaraat-Gol alkaline rocks (red diamonds) and in similar Early Paleozoic intrusions from the Sangilen Plateau, SE Tuva [51]: (a) Th/Yb–Ta/Yb diagram [52]. OIB = ocean island basalts, ACM = active continental margin, WPVZ = within-plate volcanic zone, WPB = within-plate basalts, E-MORB = “enriched-type” mid-ocean ridge basalts; (b)  $Th_N$ – $Nb_N$  diagram [53]. AB = alkali basalt, BAB = back-arc basin basalt; N-MORB-normalized Th and Nb [31]; (c) Nb/Y–Zr/Y diagram [54]: ARC = island arc basalt, OPB = oceanic plateau basalt, N-MORB = “normal-type” mid-ocean ridge basalt, IAB = island arc basalt. Crosses and white star in panels (b,c), respectively, mark average compositions of oceanic basalts [31,32]; (d) Rb–(Y + Nb) diagram [55]. syn-COLG = collision granites, VAG = volcanic arc granites, WPG = within-plate granites.

Alkaline magmatism with such signatures apparently evolved in a setting of active continental-margin distributed rifting, like the Basin and Range Province in California. Repeated formation of mantle magma centers during the early CAOB history supports the idea of periodic plume-related activity during the Paleozoic [56]. The synchronicity of the Cambrian–Early Ordovician, Early–Middle Devonian, Late Carboniferous–Permian, and (partly) Early Triassic events of high-alkali magmatism in the western CAOB over the ~520–260 Ma time span with periods of plume activity (Figure 6) may be evidence of cyclic mantle processes. According to the new U–Pb data, the Overmaraat-Gol pluton in Northern Mongolia resulted from an Early Silurian (Wenlock, ~426 Ma) event of alkaline magmatism which was the final phase (“last echo”) of the North-Asian plume.

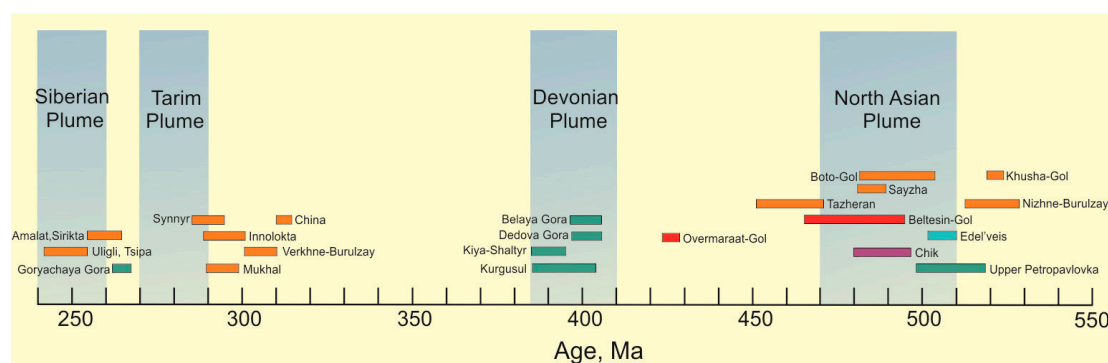


**Figure 6.** Correlation between plume activity events and pluton ages: Plutons of the alkaline provinces are shown according to published evidence [5,8,12,14–16,33,38,57–60] and our unpublished data. Igneous provinces are shown by different colors: Red for Northern Mongolia; green for Kuznetsk Alatau; orange for Baikal; blue for Russian Altai; purple for SE Tuva.

## 6. Concluding Remarks

The obtained Wenlock isotope age of the Overmaraat-Gol pluton indicates that alkaline magmatism in the western CAO had a long history. The earliest intrusions, along with Devonian and Permian–Triassic events, may have been associated with the activity of the Early Paleozoic North-Asian mantle plume. The isotope systematics and trace-element chemistry of the Overmaraat-Gol rocks suggest a multi-component source of their parent alkaline-mafic magma, which comprised mixed components of depleted and enriched mantle, as well as an inhomogeneous substrate of continental crust. As in the case of some other derivatives of Early Paleozoic alkaline magmatism in the CAO, magma may have emplaced during interaction of a mantle plume with accretionary-collisional complexes that formed previously on the active margin of the Paleoasian ocean.

**Author Contributions:** V.V.V.: Methodology, investigation, data curation, funding acquisition, project administration, writing and original draft preparation, review, and editing. I.F.G.: Resources, investigation, funding acquisition, and project administration. R.E.E.: Project administration, resources, writing, review, and editing. A.E.I.: Resources, validation, writing, review and editing. A.V.V.: Resources.

**Funding:** The geochronological work was supported by grant No. 5.8988.2017/6.7 from the Russian Ministry of Science and Higher Education to V.V.V. Geochemical investigations were conducted under financial aid from grant No. 18-17-00240 from the Russian Science Foundation to I.F.G., R.E.E., A.E.I., and A.V.V.

**Acknowledgments:** We wish to express our sincere thanks to C. Munhtogto for helping us in the field and for providing valuable samples. We are grateful to our colleagues from the National Research Tomsk State University (Tomsk), the Institute of Geology and Mineralogy (Novosibirsk), the Geological Institute of Kola Science Centre (Apatity), and the Center of Isotope Studies of the A.P. Karpinsky Russian Geological Research Institute (St. Petersburg) for their aid in analytical work. The manuscript profited from constructive criticism by three anonymous reviewers.

**Conflicts of Interest:** The authors declare no conflict of interest.

## References

1. Condi, K.C. *Mantle Plumes and Their Record in Earth History*; Cambridge University Press: Cambridge, UK, 2001; pp. 1–305.
2. Ernst, R.E. *Large Igneous Provinces*; Cambridge University Press: Cambridge, UK, 2014; pp. 1–630.
3. Pokrovskii, B.G.; Andreeva, E.D.; Vrublevskii, V.V.; Grinev, O.M. Contamination mechanisms of alkaline-gabbro intrusions in the southern periphery of the Siberian craton: Evidence from strontium and oxygen isotopic compositions. *Petrologiya* **1998**, *6*, 237–251.
4. Nikiforov, A.V.; Yarmolyuk, V.V.; Kovalenko, V.I.; Ivanov, V.G.; Zhuravlev, D.Z. Late Mesozoic carbonatites of western Transbaikalia: Isotopic–geochemical characteristics and sources. *Petrologiya* **2002**, *10*, 146–164.

5. Doroshkevich, A.G.; Ripp, G.S.; Izbrodin, I.A.; Savatenkov, V.M. Alkaline magmatism of the Vitim province, West Transbaikalia, Russia: Age, mineralogical, geochemical and isotope (O, C, D, Sr and Nd) data. *Lithos* **2012**, *152*, 157–172. [[CrossRef](#)]
6. Vrublevskii, V.V. Sources and geodynamic setting of petrogenesis of the Middle Cambrian Upper Petropavlovka alkaline basic pluton (Kuznetsk Alatau, Siberia). *Russ. Geol. Geophys.* **2015**, *56*, 379–401. [[CrossRef](#)]
7. Vrublevskii, V.V.; Krupchatnikov, V.I.; Izokh, A.E.; Gertner, I.F. The alkaline and carbonatitic rocks of Gorny Altai (Edel'veis complex) as indicators of Early Paleozoic plume magmatism in the Central Asian Fold Belt. *Russ. Geol. Geophys.* **2012**, *53*, 721–735. [[CrossRef](#)]
8. Vrublevskii, V.V.; Grinev, O.M.; Izokh, A.E.; Travin, A.V. Geochemistry, isotope triad (Nd–Sr–O), and  $^{40}\text{Ar}$ – $^{39}\text{Ar}$  age of Paleozoic alkaline mafic intrusions of the Kuznetsk Alatau (by the example of the Belaya Gora pluton). *Russ. Geol. Geophys.* **2016**, *57*, 592–602. [[CrossRef](#)]
9. Vrublevskii, V.V.; Gertner, I.F.; Chugaev, A.V. Parental sources of high-alumina alkaline melts: Nd, Sr, Pb, and O isotopic evidence from the Devonian Kiya–Shaltyr gabbro–urtite intrusion, South Siberia. *Doklady Earth Sci.* **2018**, *479*, 518–523. [[CrossRef](#)]
10. Vrublevskii, V.V.; Morova, A.A.; Bukharova, O.V.; Konovalenko, S.I. Mineralogy and geochemistry of Triassic carbonatites in the Matcha alkaline intrusive complex (Turkestan–Alai Ridge, Kyrgyz Southern Tien Shan), SW Central Asian orogenic belt. *J. Asian Earth Sci.* **2018**, *153*, 252–281. [[CrossRef](#)]
11. Vrublevskii, V.V.; Nikiforov, A.V.; Sugorakova, A.M.; Kozulina, T.V. Mantle-crustal origin of Early Paleozoic alkaline intrusions from Central Sangilen, SE Tuva: Nd, Sr, Pb, C, O isotope data. *Russ. Geol. Geophys.* **2019**, *60*. in press.
12. Vrublevskii, V.V.; Gertner, I.F.; Gutiérrez-Alonso, G.; Hofmann, M.; Grinev, O.M.; Tishin, P.A. Isotope (U–Pb, Sm–Nd, Rb–Sr) geochronology of alkaline basic plutons of the Kuznetsk Alatau. *Russ. Geol. Geophys.* **2014**, *55*, 1264–1277. [[CrossRef](#)]
13. Yashina, R.M. *Alkaline Magmatism in Orogenic Areas (Case of the Southern Periphery of the Siberian Craton)*; Nauka: Moscow, Russia, 1982; pp. 1–274. (In Russian)
14. Salnikova, E.B.; Stifeeva, M.V.; Nikiforov, A.V.; Yarmolyuk, V.V.; Kotov, A.B.; Anisimova, I.V.; Sugorakova, A.M.; Vrublevskii, V.V. Andradite–morimotoite garnets as promising U–Pb geochronometers for dating ultrabasic alkaline rocks. *Doklady Earth Sci.* **2018**, *480*, 778–782. [[CrossRef](#)]
15. Izbrodin, I.A.; Doroshkevich, A.G.; Rampilov, M.O.; Ripp, G.S.; Lastochkin, E.I.; Khubanov, V.B.; Posokhov, V.F.; Vladykin, N.V. Age and mineralogical and geochemical parameters of rocks of the China alkaline massif (western Transbaikalia). *Russ. Geol. Geophys.* **2017**, *58*, 903–921. [[CrossRef](#)]
16. Sklyarov, E.V.; Fedorovsky, V.S.; Kotov, A.B.; Lavrenchuk, A.V.; Mazukabzov, A.M.; Levitsky, V.I.; Sal'nikova, E.B.; Starikova, A.E.; Yakovleva, S.Z.; Anisimova, I.V.; et al. Carbonatites in collisional settings and pseudo-carbonatites of the Early Paleozoic Ol'khon collisional system. *Russ. Geol. Geophys.* **2009**, *50*, 1091–1106. [[CrossRef](#)]
17. Andreeva, E.D.; Yashina, R.M.; Garam, D. Nepheline rocks of Northern Mongolia. In *The Evolution of Geological Processes and Metallogeny of Mongolia*; Dergunov, A.B., Kovalenko, V.I., Eds.; Nauka: Moscow, Russia, 1990; pp. 151–165. (In Russian)
18. Yarmolyuk, V.V.; Kovalenko, V.I. Deep geodynamics and mantle plumes: Their role in the formation of the Central Asian orogenic belt. *Petrology* **2003**, *11*, 504–531.
19. Şengör, A.C.; Natal'in, B.A.; Burtman, V.S. Evolution of the Altaid tectonic collage and Palaeozoic crustal growth in Eurasia. *Nature* **1993**, *364*, 299–306. [[CrossRef](#)]
20. Jahn, B.-M.; Wu, F.Y.; Chen, B. Massive granitoid generation in Central Asia: Nd isotope evidence and implication for continental growth in the Phanerozoic. *Episodes* **2000**, *23*, 82–92.
21. Yashina, R.M.; Garam, D. Alkaline rocks of the Northern Mongolia as a possible source of nepheline and nepheline-feldspar raw materials. In *Nepheline Raw Materials*; Petrov, V.P., Ed.; Nauka: Moscow, Russia, 1978; pp. 143–152. (In Russian)
22. Kuzmichev, A.B. *Tectonic History of the Tuva-Mongolia Block: Early Baikalian, Late Baikalian and Early Caledonian Stages*; Probel: Moscow, Russia, 2004; pp. 1–192. (In Russian)
23. Williams, I.S. U–Th–Pb geochronology by ion microprobe. Applications of microanalytical techniques to understanding mineralizing processes. *Rev. Econ. Geol.* **1998**, *7*, 1–35.

24. Ludwig, K.R. *SQUID 1.00. A User's Manual*; Berkley Geochronology Center Special Publication: Berkeley, CA, USA, 2000; Volume 2, pp. 1–19.
25. Black, L.P.; Kamo, S.L.; Allen, C.M.; Aleinikoff, J.N.; Davis, D.W.; Korsch, R.J.; Foudoulis, C. TEMORA 1: A new zircon standard for U–Pb geochronology. *Chem. Geol.* **2003**, *200*, 155–170. [[CrossRef](#)]
26. Ludwig, K.R. User's Manual for Isoplot/Ex, Version 2.10. In *A Geochronological Toolkit for Microsoft Excel*; Berkley Geochronology Center Special Publication: Berkeley, CA, USA, 1999; Volume 1, pp. 1–46.
27. Bayanova, T.B. *The Age of Marker Geological Complexes of the Kola Region and Duration of Magmatic Events*; Nauka: St-Petersburg, Russia, 2004; pp. 1–174. (In Russian)
28. Faure, G. *Principles of Isotope Geology*; John Wiley & Sons: New York, NY, USA, 1986; pp. 1–608.
29. Middlemost, E.A.K. Naming materials in the magma/igneous rock system. *Earth-Sci. Rev.* **1994**, *37*, 215–244. [[CrossRef](#)]
30. De la Roche, H.; Leterrier, J.; Grandclaude, P.; Marchal, M. A classification of volcanic and plutonic rocks using R<sub>1</sub>–R<sub>2</sub> diagram and major element analyses—Its relationships with current nomenclature. *Chem. Geol.* **1980**, *29*, 183–210. [[CrossRef](#)]
31. Sun, S.; McDonough, W.F. Chemical and isotopic systematics of oceanic basalts: Implications for mantle composition and processes. In *Magmatism in the Ocean Basins*; Saunders, A.D., Norry, M.J., Eds.; Geological Society: London, UK, 1989; Volume 42, pp. 313–345.
32. Kelemen, P.B.; Hanghøj, K.; Greene, A.R. One view of the geochemistry of subduction-related magmatic arcs, with an emphasis on primitive andesite and lower crust. In *Treatise on Geochemistry*; Holland, Y.D., Turekian, K.K., Eds.; Elsevier Ltd.: Amsterdam, The Netherlands, 2003; Volume 3, pp. 593–659.
33. Vrublevskii, V.V.; Gertner, I.F. Isotopic (Nd–Sr–Pb–O) hierarchy of Paleozoic alkaline–mafic intrusions of the Kuznetsk Alatau mountains. In *Petrology of Magmatic and Metamorphic Complexes*; Ernst, R.E., Ed.; Tomsk CSTI Publishing House: Tomsk, Russia, 2018; pp. 84–91.
34. Vorontsov, A.A.; Fedoseev, G.S.; Andryushchenko, S.V. Devonian volcanism in the Minusa basin in the Altai–Sayan area: Geological, geochemical, and Sr–Nd isotopic characteristics of rocks. *Russ. Geol. Geophys.* **2013**, *54*, 1001–1025. [[CrossRef](#)]
35. Vrublevskii, V.V.; Nikiforov, A.V.; Sugorakova, A.M.; Lykhin, D.A. Isotope (Nd, Sr, Pb, O) composition of alkaline rocks from the Sangilen upland, SE Tuva. In *Geodynamical Evolution of the Central Asian Mobile Belt Lithosphere*; Sklyarov, E.V., Ed.; Institute of Earth Crust SB RAS: Irkutsk, Russia, 2014; pp. 65–67.
36. Nikiforov, A.V.; Sal'nikova, E.B.; Sugorakova, A.M.; Polyakov, N.A.; Khertek, A.K. Late Paleozoic magmatism of the Sangilen (Eastern Tuva). In *Geology, Magmatism and Metallogeny of Central Asia, Proceedings of the Ore-Magmatic Systems of the Sangilen (Alkaline Intrusives, Carbonatites), Kyzyl, Russia, 14–30 July 2018*; Mongush, A.A., Ed.; TuvIENR SB RAS: Kyzyl, Russia, 2018; pp. 84–88.
37. Vladykin, N.V.; Morikiyo, T.; Miyazaki, T. Sr and Nd isotopes geochemistry of alkaline and carbonatite complexes of Siberia and Mongolia and some geodynamic implications. In *Sources of Deep Magmatism and Plumes*; Vlagykin, N.V., Ed.; Institute of Geography: Irkutsk, Russia, 2005; pp. 19–37. (In Russian)
38. Izokh, A.E.; Polyakov, G.V.; Shelepaev, R.A.; Vrublevskii, V.V.; Egorova, V.V.; Rudnev, S.N.; Lavrenchuk, A.V.; Borodina, E.V.; Oyunchimeg, T. Early Paleozoic Large Igneous Province of the Central Asia Mobile Belt. 2008. Available online: <http://www.largeigneousprovinces.org/08may> (accessed on 10 March 2019).
39. Vrublevskii, V.V.; Voitenko, N.N.; Romanov, A.P.; Polyakov, G.V.; Izokh, A.E.; Gertner, I.F.; Krupchatnikov, V.I. Magma sources of Triassic lamproites of Gornyi Altai and Taimyr: Sr and Nd isotope evidence for plume–lithosphere interaction. *Doklady Earth Sci.* **2005**, *405A*, 1365–1367.
40. Baatar, M.; Ochir, G.; Kynicky, J.; Iizumi, S.; Comin-Chiaramonti, P. Some notes on the Lugiin Gol, Mushgai Khudag and Bayan Khoshuu alkaline complexes, Southern Mongolia. *Int. J. Geosci.* **2013**, *4*, 1200–1214. [[CrossRef](#)]
41. Krupchatnikov, V.I.; Vrublevskii, V.V.; Kruk, N.N. Early Mesozoic lamproites and monzonitoids of southeastern Gornyi Altai: Geochemistry, Sr–Nd isotope composition, and sources of melts. *Russ. Geol. Geophys.* **2015**, *56*, 825–843. [[CrossRef](#)]
42. Lightfoot, P.C.; Hawkesworth, C.J.; Hergt, J.; Naldrett, A.J.; Gorbachev, N.S.; Fedorenko, V.A.; Doherty, W. Remobilisation of the major-, trace-element, and from picritic and tholeiitic Siberian Trap, Russia. *Contrib. Miner. Petrol.* **1993**, *114*, 171–188. [[CrossRef](#)]
43. Zindler, A.; Hart, S.R. Chemical geodynamics. *Annu. Rev. Earth Planet. Sci.* **1986**, *14*, 493–571. [[CrossRef](#)]

44. Stracke, A.; Hofmann, A.W.; Hart, S.R. FOZO, HIMU, and the rest of the mantle zoo. *Geochem. Geophys. Geosyst.* **2005**, *6*, Q05007. [[CrossRef](#)]
45. Xu, X.S.; Zhang, M.; Zhu, K.Y.; Chen, X.M.; He, Z.Y. Reverse age zonation of zircon formed by metamictisation and hydrothermal fluid leaching. *Lithos* **2012**, *150*, 256–267. [[CrossRef](#)]
46. Vrublevskii, V.V.; Kotel'nikov, A.D.; Rudnev, S.N.; Krupchatnikov, V.I. Evolution of the Paleozoic granitoid magmatism in the Kuznetsk Alatau: New geochemical and U-Pb (SHRIMP-II) isotope data. *Russ. Geol. Geophys.* **2016**, *57*, 225–246. [[CrossRef](#)]
47. Rudnev, S.N. *Early Paleozoic Granitoid Magmatism in the Altai-Sayan Folded Area and in the Lake Zone in Western Mongolia*; Publishing SB RAS: Novosibirsk, Russia, 2013; pp. 1–300. (In Russian)
48. Bell, K.; Tilton, G.R. Nd, Pb and Sr isotopic compositions of East African carbonatites: Evidence for mantle mixing and plume inhomogeneity. *J. Petrol.* **2001**, *42*, 1927–1945. [[CrossRef](#)]
49. Bell, K.; Lavecchia, G.; Rosatelli, G. Cenozoic Italian magmatism—Isotope constraints for possible plume-related activity. *J. S. Am. Earth Sci.* **2013**, *41*, 22–40. [[CrossRef](#)]
50. Vrublevskii, V.V.; Kotel'nikov, A.D.; Izokh, A.E. The age and petrologic and geochemical conditions of formation of the Kogtakh gabbro-monzonite complex in the Kuznetsk Alatau. *Russ. Geol. Geophys.* **2018**, *59*, 718–744. [[CrossRef](#)]
51. Vrublevskii, V.V.; Nikiforov, A.V.; Sugorakova, A.M.; Kozulina, T.V. Geochemistry and petrogenesis of the Kharly carbonatite-alkaline complex (Sangilen Plateau, Southern Siberia): Implications for Early Paleozoic magma sources and tectonic settings in the Western Central Asian Orogenic Belt. *Lithos* **2019**, under review.
52. Gorton, M.P.; Schandl, E.S. From continents to island arcs: A geochemical index of tectonic setting for arc-related and within-plate felsic to intermediate volcanic rocks. *Can. Miner.* **2000**, *38*, 1065–1073. [[CrossRef](#)]
53. Saccani, E. A new method of discriminating different types of post-Archean ophiolitic basalts and their tectonic significance using Th–Nb and Ce–Dy–Yb systematics. *Geosci. Front.* **2015**, *6*, 481–501. [[CrossRef](#)]
54. Condie, K.C. High field strength element ratios in Archean basalts: A window to evolving sources of mantle plumes? *Lithos* **2005**, *79*, 491–504. [[CrossRef](#)]
55. Pearce, J.A.; Harris, N.B.W.; Tindle, A.G. Trace element discrimination diagrams for the tectonic interpretation of granitic rocks. *J. Petrol.* **1984**, *25*, 956–983. [[CrossRef](#)]
56. Yarmolyuk, V.V.; Kovalenko, V.I.; Kovach, V.P.; Kozakov, I.K.; Kotov, A.B.; Sal'nikova, E.B. Geodynamics of caledonides in the Central Asian foldbelt. *Doklady Earth Sci.* **2003**, *389A*, 311–316.
57. Vrublevskii, V.V.; Gertner, I.F.; Zhuravlev, D.Z.; Makarenko, N.A. The Sm–Nd isotopic age and source of comagmatic alkaline mafic rocks and carbonatites of Kuznetsk Alatau. *Doklady Earth Sci.* **2003**, *391A*, 832–835.
58. Nikiforov, A.V.; Yarmolyuk, V.V. Early Paleozoic age and geodynamic setting of the Botogol and Khushagol alkaline massifs in the Central Asian fold belt. *Doklady Earth Sci.* **2007**, *412*, 6–10. [[CrossRef](#)]
59. Vrublevskii, V.V.; Izokh, A.E.; Polyakov, G.V.; Gertner, I.F.; Yudin, D.S.; Krupchatnikov, V.I. Early Paleozoic alkaline magmatism of the Altai Mountains:  $^{40}\text{Ar}$ – $^{39}\text{Ar}$  geochronology data for the Edel'veis complex. *Doklady Earth Sci.* **2009**, *427*, 846–850. [[CrossRef](#)]
60. Doroshkevich, A.G.; Izbrodin, I.A.; Rampilov, M.O.; Ripp, G.S.; Lastochkin, E.I.; Khubanov, V.B. Permo–Triassic stage of alkaline magmatism in the Vitim plateau (western Transbaikalia). *Russ. Geol. Geophys.* **2018**, *59*, 1061–1077. [[CrossRef](#)]

